

Nonlinear Thermoelectricity with Electron-Hole Symmetric Systems

G. Marchegiani^{✉,*}, A. Braggio^{✉,†}, and F. Giazotto^{✉,‡}

NEST Istituto Nanoscienze-CNR and Scuola Normale Superiore, I-56127 Pisa, Italy



(Received 10 September 2019; revised manuscript received 5 February 2020; accepted 14 February 2020; published 10 March 2020)

In the linear regime, thermoelectric effects between two conductors are possible only in the presence of an explicit breaking of the electron-hole symmetry. We consider a tunnel junction between two electrodes and show that this condition is no longer required outside the linear regime. In particular, we demonstrate that a thermally biased junction can display an absolute negative conductance, and hence thermoelectric power, at a small but finite voltage bias, provided that the density of states of one of the electrodes is gapped and the other is monotonically decreasing. We consider a prototype system that fulfills these requirements, namely, a tunnel junction between two different superconductors where the Josephson contribution is suppressed. We discuss this nonlinear thermoelectric effect based on the spontaneous breaking of electron-hole symmetry in the system, characterize its main figures of merit, and discuss some possible applications.

DOI: 10.1103/PhysRevLett.124.106801

Introduction.—Recently, thermal transport at the nano-scale and the field of quantum thermodynamics have attracted growing interest [1–14]. In particular, thermoelectric systems have been extensively investigated [15–26], since they provide a direct thermal-to-electrical power conversion. In a two-terminal system, a necessary condition for thermoelectricity in the linear regime, i.e., for a small voltage V and a small temperature bias ΔT , is breaking the electron-hole (EH) symmetry which results in the transport property $I(V, \Delta T) \neq -I(-V, \Delta T)$, where I is the charge current flowing through the two-terminal system. In fact, if $I(V, \Delta T) = -I(-V, \Delta T)$, it follows $I(0, \Delta T) = 0$, and hence a null thermopower, irrespectively of the temperature bias ΔT . Nonlinear thermoelectric effects have also been investigated [27–35], even in systems where $I(0, \Delta T) = 0$ [36], but the EH symmetry breaking is always assumed. For metals, the EH symmetry is roughly present for Landau-Fermi liquids at small energies, and indeed thermoelectric effects in real metals are typically small, scaling as T/T_F , where T_F is the Fermi temperature. More generally, a nearly perfect EH symmetry characterizes many interacting systems in the quantum regime, such as superconductors [37,38] or Dirac materials [39].

Here, we establish a set of sufficient and universal conditions for finite thermoelectric power $\dot{W} = -IV > 0$ in systems where EH symmetry holds, $I(V, \Delta T) = -I(-V, \Delta T)$. More precisely, we demonstrate that the electron-hole symmetry breaking which leads to thermoelectricity is driven by the nonlinear temperature difference and asymmetry between the two terminals.

Model.—We consider a basic example in quantum transport, namely, a tunnel junction, which is also experimentally relevant. The system consists of two conducting electrodes (L, R), coupled through a thin insulating barrier,

where quantum tunneling takes place. In this case, the main contribution to transport is typically given by Landau’s fermionic excitations, called quasiparticles. For the purpose of our discussion, we assume each electrode in internal thermal equilibrium, namely, the quasiparticle distributions read $f_\alpha(E - \mu_\alpha) = \{1 + \exp[(E - \mu_\alpha)/(k_B T_\alpha)]\}^{-1}$, where k_B is the Boltzmann constant and T_α, μ_α (with $\alpha = L, R$) are the temperatures and the chemical potentials of the quasiparticle systems, respectively. The quasiparticle charge and heat current flowing out of the α electrode (with $\bar{\alpha} = R$ when $\alpha = L$ and vice versa) read [37,40]

$$\begin{pmatrix} I_\alpha \\ \dot{Q}_\alpha \end{pmatrix} = \frac{G_T}{e^2} \int_{-\infty}^{+\infty} dE \begin{pmatrix} -e \\ E \end{pmatrix} N_\alpha(E_\alpha) N_{\bar{\alpha}}(E_{\bar{\alpha}}) F_\alpha(E_\alpha), \quad (1)$$

where $-e$ is the electron charge, $N_\alpha(E)$ is the quasiparticle density of states (DOS), $F_\alpha(E_\alpha) = f_\alpha(E_\alpha) - f_{\bar{\alpha}}(E_{\bar{\alpha}})$, $E_\alpha = E - \mu_\alpha$, and G_T is the conductance of the junction if both the electrodes have constant N_α . For simplicity, we assumed spin degeneracy and an energy and spin independent tunneling in the derivation of Eq. (1). We consider EH symmetric DOSs, $N_\alpha(E) = N_\alpha(-E)$, and we define $I = I_L$ [41]. Under a voltage bias $V \neq 0$, the chemical potentials are shifted: $\mu_L - \mu_R = -eV$. By exploiting the symmetries, one can show that $I(V, T_L, T_R) = -I(-V, T_L, T_R)$ and $\dot{Q}_\alpha(V, T_L, T_R) = \dot{Q}_\alpha(-V, T_L, T_R)$ [42]. The expressions of Eq. (1) respect the thermodynamic laws [1,34,48,49]. In particular, the energy conservation in the junction reads $\dot{Q}_L + \dot{Q}_R + IV = 0$ (first law), and the entropy production rate $\dot{S} = -\dot{Q}_L/T_L - \dot{Q}_R/T_R$ is not negative (second law) [1,34,50]. As a consequence, for $T_L = T_R = T$ it follows $IV \geq 0$. Conversely, for $T_L \neq T_R$, the condition $IV < 0$ is possible. For instance,

in a thermoelectric generator, the condition $\dot{W} = -IV > 0$ is thermodynamically consistent with the constraint $\dot{S} \geq 0$ if the efficiency of the conversion $\eta = \dot{W}/\dot{Q}_{\text{hot}}$ is not larger than the Carnot efficiency, $\eta \leq \eta_C = 1 - T_{\text{cold}}/T_{\text{hot}}$ ($\dot{Q}_{\text{hot}} > 0$ is the heat current from the hot lead).

Consider the charge current I from Eq. (1). Essentially, the condition on the existence of a thermoelectric power $\dot{W} > 0$ can be expressed as the possibility of having an absolute negative conductance (ANC), $I(V)/V < 0$, under a thermal bias. Thanks to EH symmetry, we can focus on $V > 0$ and ask whether we can have $I(V, T_L, T_R) < 0$ for $T_L \neq T_R$. With no loss of generality, we assume here and in the rest of this work $T_L \geq T_R$, with $\Delta T = T_L - T_R$. For $N_L(E) = N_R(E)$, one can prove that $I(V) \geq 0$ for $V > 0$; namely, two *different* DOSs are necessary for thermoelectricity in the presence of EH symmetry [42]. Our goal is to derive sufficient conditions on the two DOSs which guarantee the existence of thermoelectricity.

To this end, it is convenient to measure the energy E with respect to μ_L ; i.e., we set $\mu_L = 0$, $\mu_R = eV$. We rewrite, with simple manipulations, the charge current I of Eq. (1) as

$$I = \frac{G_T}{e} \int_0^\infty dE N_L(E) f_L(E) [N_R(E_+) - N_R(E_-)] + \frac{G_T}{e} \int_0^\infty dE N_L(E) [N_R(E_-) f_R(E_-) - N_R(E_+) f_R(E_+)], \quad (2)$$

where $E_\pm = E \pm eV$. If N_L is a gapped function (with gap Δ_L), that is, $N_L \approx 0$ for $|E| < \Delta_L$, the second term in Eq. (2) is negligible when $eV, k_B T_R \ll \Delta_L$, due to the exponential damping of the cold distribution f_R above the gap Δ_L . Moreover, for $k_B T_L \sim \Delta_L$, the integrand function in the first term of Eq. (2) is finite, owing to the presence of the hot distribution f_L , and negative when $N_R(E)$ is a monotonically decreasing function for $E > \Delta_L - eV$. In conclusion, even with EH symmetric DOSs, the presence of a gap in the hot electrode DOS and the monotonically decreasing function in the cold electrode DOS may generate an ANC, and hence thermoelectricity $\dot{W} = -IV > 0$. This is the crucial result of this work, and can be applied in a quite general setting [42]. Below, we discuss the main features of this nonlinear thermoelectric effect for an experimentally suitable EH symmetric system: a tunnel junction between two Bardeen-Cooper-Schrieffer (BCS) superconductors (*S-I-S* junction).

S-I-S junction.—For simplicity, we focus on quasiparticle transport and assume to completely suppress the Josephson contribution occurring in *S-I-S* junctions [8,52,53]. This condition can be achieved either by considering a junction with a strongly oxidized barrier or by appropriately applying an external in-plane magnetic field. The quasiparticle DOS reads $N_\alpha = \theta(|E| - \Delta_\alpha) |E| / \sqrt{E^2 - \Delta_\alpha^2}$ [54], where $\Delta_\alpha(T_\alpha)$ are the temperature

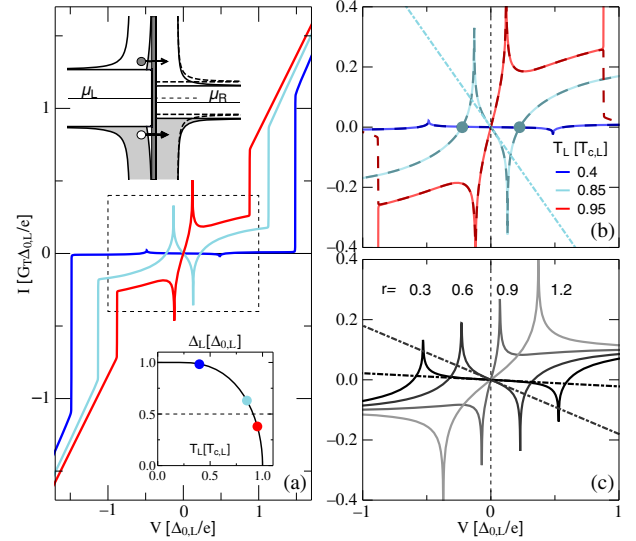


FIG. 1. (a) Quasiparticle current-voltage characteristic of a thermally biased tunnel junction between two superconductors (*S-I-S* junction) for $T_R = 0.01 T_{c,L}$, $r = 0.5$ and different values of $T_L > T_R$. The curves display absolute negative conductance (ANC) and thermoelectric power $\dot{W} = -IV > 0$ at small voltage bias if $\Delta_L(T_L) > \Delta_{0,R}$. Top inset: Energy band diagram of the *S-I-S* junction. The combination of the gap in the hot electrode (left) and the monotonically decreasing DOS above gap of the cold electrode (right) produces a particle current which flows in the opposite direction of the chemical potential gradient. Bottom inset: Temperature dependence of the superconducting gap Δ_L . Colored points mark the values of $\Delta_L(T_L)$ for the curves displayed in (a). The horizontal dashed line intercepts the Δ_L curve at the point where $\Delta_L(T_L) = \Delta_{0,R}$, i.e., the maximum temperature for the existence of the ANC in (a) and (b). (b) Enlargement of the subgap transport in (a) (dashed rectangle). Dashed curves give the first term of Eq. (2). The light blue dots give the values of the Seebeck voltage V_S . (c) Subgap IV characteristics for $T_L = 0.7 T_{c,L}$, $T_R = 0.01 T_{c,L}$, and different values of r . The slopes of the dash-dotted lines in (b) and (c) give the values of the ANC at $V \approx 0$, as expressed by Eq. (3).

dependent superconducting order parameters. In particular, $\Delta_\alpha(T_\alpha = 0) = \Delta_{0,\alpha}$ and it decreases monotonically with T_α , following a universal relation, obtained through a self-consistent calculation [37] [see the bottom inset of Fig. 1(a)]. It becomes zero when the temperature approaches the critical value $T_{c,\alpha} = \Delta_{0,\alpha}/(1.764 k_B)$. We stress that the temperature dependence of Δ_α is not necessary for the mechanism, and it is characteristic of the specific system considered here.

Since $N_L(E) \neq N_R(E)$ is a necessary condition for thermoelectricity, hereafter we consider the case where the two gaps at zero temperature differ, introducing a parameter $r = \Delta_{0,R}/\Delta_{0,L} = T_{c,R}/T_{c,L}$.

Consider now Eq. (2) for a *S-I-S* junction. As discussed above, for $eV, k_B T_R \ll \Delta_L(T_L)$ the second term is negligible and $I(V)$ is given entirely by the first contribution. To have ANC, two conditions must apply: (i) the hot

temperature T_L must be of the order of the gap, $k_B T_L \lesssim \Delta_L(T_L)$, due to the presence of $f_L(E)$ (but necessarily smaller than $T_{c,L}$ for the superconductivity to survive), and (ii) the term in the square bracket must be negative. Since the BCS DOS $N_R(E)$ is monotonically decreasing only for $E > \Delta_R(T_R)$, the two conditions require $\Delta_L(T_L) - \Delta_R(T_R) > 0$. Being $\Delta_L(T_L)$ a monotonically decreasing function, the conditions are met only if the hot superconductor has the larger gap. Thus, a necessary condition for ANC is $r < 1$ when $T_L > T_R$. Conversely, by inverting the temperature gradient, i.e., $T_R > T_L$, the thermoelectricity requires $\Delta_R(T_R) - \Delta_L(T_L) > 0$ and the proper conditions are met for $r > 1$. The origin of the thermoelectricity can be intuitively understood in the energy band diagram in the top inset of Fig. 1(a), drawn for $T_L > T_R$ and $\mu_L > \mu_R$. The net current is given by the difference of the particle (fill circle) and the holes (empty circle) contributions. They exactly cancel out at $V = 0$, due to EH symmetry. For $V \neq 0$, the shifting of N_R decreases (increases) the particles (holes) contribution, due to locally monotonic decreasing behavior. As a consequence, the particle current flows in the opposite direction of the chemical potential gradient.

Figure 1(a) displays the IV characteristics for $r = 0.5$, $T_R = 0.01T_{c,L}$, and different values of $T_L > T_R$. The evolution is linear $I \simeq G_T V$ at large bias $eV > \Delta_L(T_L) + \Delta_R(T_R)$ and strongly nonlinear within the gap, i.e., for $eV < \Delta_L(T_L) + \Delta_R(T_R)$. Figure 1(b) gives an enlarged view of the subgap transport displayed in Fig. 1(a) (dashed rectangle). Within the gap, the curves display characteristic peaks at $eV_{\text{peak}} = \pm |\Delta_L(T_L) - \Delta_R(T_R)| \sim \pm |\Delta_L(T_L) - \Delta_{0,R}|$, due to the matching of the BCS singularities in the DOSs. Interestingly, the curves display a significant ANC, and hence thermoelectricity, for intermediate values of T_L . Furthermore, the thermoelectric effect is negligible if $\Delta T = T_L - T_R$ is too low and it is absent when $\Delta_L(T_L) < \Delta_R(T_R)$. The contributions due to the first term of Eq. (2) are displayed with dashed lines in Fig. 1(b). As argued above, they yield a good approximation for $eV < \Delta_L$. The dependence of the IV characteristics on r is visualized in Fig. 1(c) for $T_L = 0.7T_{c,L} > T_R = 0.01T_{c,L}$. In particular, the ANC is present only when $\Delta_{0,R} < \Delta_L(T_L) \sim 0.83\Delta_{0,L}$, namely for $r \lesssim 0.83$.

For $V \sim 0$, the IV characteristic is approximately linear and, by using the first term of Eq. (2), we can derive an expression for the negative conductance [42], namely,

$$G_0 = \lim_{V \rightarrow 0} \frac{I(V)}{V} = -2G_T \Delta_{0,R}^2 \int_{\Delta_L(T_L)}^{\infty} dE \frac{N_L(E) f_L(E)}{(E^2 - \Delta_{0,R}^2)^{3/2}}, \quad (3)$$

valid for $T_R \ll T_{c,R}$ and $\Delta_L(T_L) > \Delta_{0,R}$. This negative slope is shown in Figs. 1(b) and 1(c) for some curves with dot-dashed lines, which perfectly represent the linear-in-bias behavior.

We stress that the existence of the ANC in a thermally biased S - I - S junction is not discussed in the literature to the best of our knowledge. This is not totally surprising, since the ANC can be observed only for $r \neq 1$ and higher temperature of the larger gap superconducting electrode $T_L \lesssim T_{c,L}$. This effect is reminiscent of the ANC predicted [56] and observed in experiments on nonequilibrium superconductivity, with particles injection [57–59] or microwave irradiation [60].

Thermoelectric figures of merit.—Because of the nonlinear nature of the effect, we cannot rely on the standard figures of merit for linear thermoelectric effects. Yet, in the nonlinear regime we can still define the Seebeck voltage V_S which corresponds to the voltage developed by the thermal bias ΔT at open circuit. Consider, for instance, the light blue curve in Fig. 1(b), where there is thermoelectricity $\dot{W} > 0$. Clearly, the curve crosses the x axis in $V = 0$, as required by EH symmetry. Furthermore, if there is ANC at low voltage ($I/V < 0$) and an Ohmic behavior at high voltage ($I/V \sim G_T > 0$), there will be, at least, two finite values $V = \pm V_S \neq 0$, where $I(V) = 0$ [see marked points in Fig. 1(b)].

Figure 2(a) displays $|V_S|$ as a function of r for $T_R = 0.01T_{c,R}$ and some values of $T_L > T_R$ (solid lines). The curves show some characteristic features: (i) for a given T_L , $|V_S|$ decreases monotonically with r and it is zero when r is larger than some critical value (depending on T_L), and

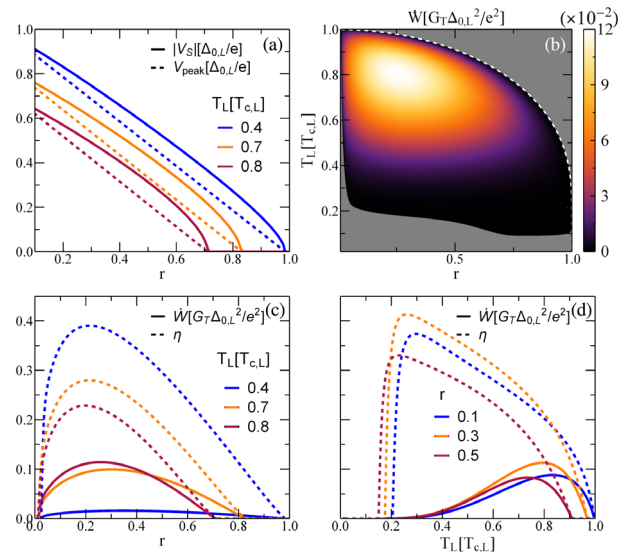


FIG. 2. Thermoelectric figures of merit for a S - I - S junction. (a) Seebeck voltage versus r for $T_R = 0.01T_{c,R}$ and some values of T_L (solid lines). The voltage corresponding to the singularity matching peak is displayed for a comparison (dashed lines). (b) Density plot of the thermoelectric power $\dot{W} = -IV$ versus r and T_L for $T_R = 0.01T_{c,L}$. In the gray region the thermoelectric effect is absent; i.e., the junction is dissipative $\dot{W} < 0$. The white dashed curve displays the equation $\Delta_L(T_L) = \Delta_{0,R}$. (c), (d) Cuts of (b) for particular values of T_L and r , respectively. The correspondent thermoelectric efficiency $\eta = \dot{W}/\dot{Q}_L$ is plotted with dashed lines.

(ii) for a given r , $|V_S|$ decreases when the temperature T_L , that is proportional to the temperature difference ΔT , is increased, something that differs with the usual linear thermoelectricity. These features can be qualitatively understood by comparing V_S with the matching peak value $V_{\text{peak}} = [\Delta_L(T_L) - \Delta_R(T_R)]/e$ [dashed curves in Fig. 2(a)]. In fact, the magnitude of V_S is correlated to V_{peak} , i.e., $|V_S| \geq V_{\text{peak}}$ when there is thermoelectricity [see Figs. 1(b) and 1(c)]. By definition, for a given T_L , V_{peak} decreases almost linearly with r ; i.e., $eV_{\text{peak}}/\Delta_{0,L} \sim \Delta_L(T_L)/\Delta_{0,L} - r$. This explains also the temperature evolution, since $\Delta_L(T_L)$ is a monotonically decreasing function. In particular, when r is larger than a critical value depending on T_L , i.e., $r \gtrsim \Delta_L(T_L)/\Delta_{0,L}$, V_S goes to zero since $\Delta_L(T_L) < \Delta_R(T_R)$, i.e., there is no thermoelectricity. For $r = 0.3$, an effective nonlinear Seebeck coefficient $\mathcal{S} = V_S/\Delta T$ can reach values as large as $\sim 0.8\Delta_{0,L}/(0.4eT_{c,L}) = 2 \times 1.764k_B/e \sim 300 \mu\text{V}/\text{K}$.

Now, we consider the thermoelectric power $\dot{W} = -IV$. For simplicity, we evaluate it at V_{peak} , where it is approximately maximum [42], namely, $-I(V_{\text{peak}})V_{\text{peak}} \sim \max_V(-IV)$. Figure 2(b) displays the density plot of \dot{W} as a function of r and T_L for $T_R = 0.01T_{c,L}$. The thermoelectric power is absent if $T_L \leq 0.1T_{c,L}$, irrespectively of r . Furthermore, it is zero when $\Delta_L(T_L) < \Delta_{0,R}$ [the dashed white line in Fig. 2(b) displays the curve $\Delta_L(T_L) = \Delta_{0,R}$]. The maximum value of \dot{W} is obtained at $r \sim 0.25$ and $T_L = 0.8T_{c,L}$ and it yields $\dot{W}_{\text{max}} \sim 0.11G_T\Delta_{0,L}^2/e^2$. For an aluminum based ($\Delta_{0,L}/e \sim 200 \mu\text{V}$) tunnel junction with $G_T = (1 \text{ k}\Omega)^{-1}$, the maximum is $\dot{W}_{\text{max}} \sim 4 \text{ pW}$.

For a better characterization, we consider cuts of Fig. 2(b) for specific values of T_L [solid curves in Fig. 2(c)] and r [solid curves in Fig. 2(d)]. In both panels, we add the corresponding thermoelectric efficiency $\eta = \dot{W}/\dot{Q}_L$ (dashed curves). Interestingly, the highest absolute efficiency with respect to r is obtained almost in correspondence of the maximum power $\eta_{\text{max}} \sim 0.4$ [see Fig. 2(c)]. Conversely, the best condition for η as a function of T_L does not coincide with the condition for maximum power [see Fig. 2(d)], although η is quite high even at the best condition in terms of power $\eta_{\dot{W}_{\text{max}}} = \eta(T_L = 0.8T_{c,L}) \sim 0.22$ [orange line in Fig. 2(d)].

Spontaneous symmetry breaking.—Here we discuss the experimental consequences of thermoelectricity in terms of the junction's dynamics. We consider a minimal circuitual setup, displayed in Fig. 3(a). The junction is modeled as a nonlinear element of characteristic $I(V, T_L, T_R)$ and capacitance C , in parallel with a load external circuit of resistance R . The evolution is obtained by requiring the current conservation in the circuit,

$$I(V, T_L, T_R) = -C\dot{V} - \frac{V}{R}, \quad (4)$$

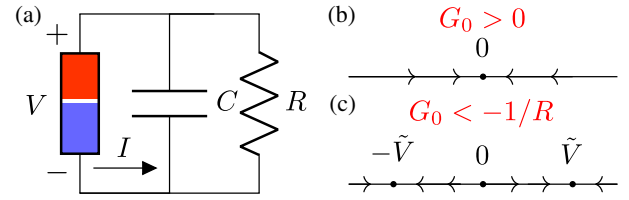


FIG. 3. (a) Circuitual scheme. The junction is a nonlinear element with characteristic $I(V, T_L, T_R)$ and capacitance C , connected to a generic load R . (b),(c) Phase portrait for the voltage dynamics across the system. (b) In the absence of thermoelectricity, $G_0 > 0$ and the voltage relaxes to 0, due to the dissipation in the load. (c) In the presence of thermoelectricity and for $G_0 < -1/R$, the zero-voltage solution is unstable and a voltage, either $\pm\tilde{V}$, spontaneously develops across the junction.

where the dot denotes the time (t) derivative. The stationary points are obtained by setting $\dot{V} = 0$ in Eq. (4) and read $V(t) = \tilde{V}$, where \tilde{V} is a solution of the implicit equation $RI(\tilde{V}, T_L, T_R) + \tilde{V} = 0$. Since $I(V, T_L, T_R) = -I(-V, T_L, T_R)$, the equation has an odd number of solutions and $\tilde{V} = 0$ is always a solution, irrespectively of R, T_L, T_R . The stability of these solutions can be acquired by linearizing Eq. (4), namely, $\dot{v} = -C^{-1}[G(\tilde{V}) + 1/R]v$, where $v = V - \tilde{V}$ and $G(\tilde{V}) = dI/dV|_{V=\tilde{V}}$. The solution is stable if the term in the square bracket is positive and unstable otherwise.

In the absence of thermoelectricity, $IV \geq 0$ and the zero-bias conductance of the junction is positive $G_0 \geq 0$. Thus, $\tilde{V} = 0$ is the unique solution of Eq. (4) and it is stable [see Fig. 3(b)]. Conversely, when we apply a temperature gradient and the S - I - S junction displays thermoelectricity, $G_0 < 0$ [see Eq. (3)], and additional solutions at finite voltages are possible. In particular, for sufficiently large values of the load, such as $R > -G_0^{-1}$, there are three solutions, $V = 0, \pm\tilde{V}$ and $G(\pm\tilde{V}) > 0$. As a consequence, any voltage signal across the device evolves toward one of the two values $\pm\tilde{V}$, depending on the initial conditions [see Fig. 3(c)]. Namely, the combination of a sufficiently strong thermal gradient and the voltage polarization imposed by the external circuit leads to a *spontaneous breaking* of EH symmetry. Moreover, the bistability of the stationary voltage may be used to design a volatile thermoelectric memory or a switch [42]. In a more general setting which includes inductive effects, the instability of the zero-voltage state can generate also a self-sustained oscillatory dynamics [42,61,62].

Conclusions.—In summary, we discussed a general thermoelectric effect occurring in systems with EH symmetry in the nonlinear regime. For a two-terminals tunneling system, two sufficient conditions are required for thermoelectricity: (i) the hot electrode has a gapped DOS and (ii) the cold electrode has a locally monotonically decreasing DOS. In particular, we investigated a prototype system: a tunnel junction between two different BCS

superconductors. We displayed the relevant figures of merit and showed that a thermoelectric voltage spontaneously develops across the system, under proper conditions. Our results may be extended to different classes of materials, including hybrid ferromagnetic-superconducting junctions or low-dimensional quantum systems (dots or wires). This work can represent a promising step in the exploration of thermoelectric effects in the nonlinear regime.

We thank Robert Whitney, David Sánchez, Tomáš Novotný, Björn Sothmann, and Giuliano Benenti for discussions and comments. We acknowledge the EU's Horizon 2020 research and innovation programme under Grant Agreement No. 800923 (SUPERTED) for partial financial support. A. B. acknowledges the CNR-CONICET cooperation program Energy conversion in quantum nanoscale hybrid devices, the Royal Society through the International Exchanges between the UK and Italy (Grants No. IES R3 170054 and No. IEC R2 192166), and the SNS-WIS joint lab QUANTRA funded by the Italian Ministry of Foreign Affairs and International Cooperation.

*giampiero.marchegiani@nano.cnr.it

†alessandro.braggio@nano.cnr.it

‡francesco.giazotto@sns.it

- [1] G. Benenti, G. Casati, K. Saito, and R. Whitney, *Phys. Rep.* **694**, 1 (2017).
- [2] Y. Dubi and M. Di Ventra, *Rev. Mod. Phys.* **83**, 131 (2011).
- [3] R. Kosloff, *Entropy* **15**, 2100 (2013).
- [4] U. Seifert, *Rep. Prog. Phys.* **75**, 126001 (2012).
- [5] J. T. Muhonen, M. Meschke, and J. P. Pekola, *Rep. Prog. Phys.* **75**, 046501 (2012).
- [6] M. Campisi, P. Hänggi, and P. Talkner, *Rev. Mod. Phys.* **83**, 771 (2011).
- [7] F. Giazotto, T. T. Heikkilä, A. Luukanen, A. M. Savin, and J. P. Pekola, *Rev. Mod. Phys.* **78**, 217 (2006).
- [8] A. Fornieri and F. Giazotto, *Nat. Nanotechnol.* **12**, 944 (2017).
- [9] N. Brunner, N. Linden, S. Popescu, and P. Skrzypczyk, *Phys. Rev. E* **85**, 051117 (2012).
- [10] A. C. Barato and U. Seifert, *Phys. Rev. Lett.* **114**, 158101 (2015).
- [11] M. Polettini, G. Verley, and M. Esposito, *Phys. Rev. Lett.* **114**, 050601 (2015).
- [12] G. Verley, M. Esposito, T. Willaert, and C. V. den Broeck, *Nat. Commun.* **5**, 4721 (2014).
- [13] P. Pietzonka and U. Seifert, *Phys. Rev. Lett.* **120**, 190602 (2018).
- [14] S. K. Manikandan, L. Dabelow, R. Eichhorn, and S. Krishnamurthy, *Phys. Rev. Lett.* **122**, 140601 (2019).
- [15] N. R. Claughton and C. J. Lambert, *Phys. Rev. B* **53**, 6605 (1996).
- [16] K. Brandner, K. Saito, and U. Seifert, *Phys. Rev. Lett.* **110**, 070603 (2013).
- [17] B. Sothmann, R. Sánchez, and A. N. Jordan, *Nanotechnol.* **26**, 032001 (2015).
- [18] A. Ozaeta, P. Virtanen, F. S. Bergeret, and T. T. Heikkilä, *Phys. Rev. Lett.* **112**, 057001 (2014).
- [19] M. Esposito, K. Lindenberg, and C. V. den Broeck, *Europhys. Lett.* **85**, 60010 (2009).
- [20] F. Vischi, M. Carrega, P. Virtanen, E. Strambini, A. Braggio, and F. Giazotto, *Sci. Rep.* **9**, 3238 (2019).
- [21] R. S. Whitney, *Phys. Rev. Lett.* **112**, 130601 (2014).
- [22] F. Giazotto, T. T. Heikkilä, and F. S. Bergeret, *Phys. Rev. Lett.* **114**, 067001 (2015).
- [23] F. Ronetti, L. Vannucci, G. Dolcetto, M. Carrega, and M. Sassetti, *Phys. Rev. B* **93**, 165414 (2016).
- [24] F. Giazotto, J. W. A. Robinson, J. S. Moodera, and F. S. Bergeret, *Appl. Phys. Lett.* **105**, 062602 (2014).
- [25] G. Marchegiani, P. Virtanen, F. Giazotto, and M. Campisi, *Phys. Rev. Applied* **6**, 054014 (2016).
- [26] M. Kamp and B. Sothmann, *Phys. Rev. B* **99**, 045428 (2019).
- [27] J. Azema, P. Lombardo, and A.-M. Daré, *Phys. Rev. B* **90**, 205437 (2014).
- [28] Y. Kim, W. Jeong, K. Kim, W. Lee, and P. Reddy, *Nat. Nanotechnol.* **9**, 881 (2014).
- [29] N. A. Zimbovskaya, *J. Chem. Phys.* **142**, 244310 (2015).
- [30] A. Svilans, A. M. Burke, S. F. Svensson, M. Leijnse, and H. Linke, *Physica (Amsterdam)* **82E**, 34 (2016).
- [31] D. Sánchez and L. Serra, *Phys. Rev. B* **84**, 201307(R) (2011).
- [32] D. Boese and R. Fazio, *Europhys. Lett.* **56**, 576 (2001).
- [33] D. Sánchez and R. López, *C. R. Phys.* **17**, 1060 (2016).
- [34] R. S. Whitney, *Phys. Rev. B* **87**, 115404 (2013).
- [35] P. A. Erdman, J. T. Peltonen, B. Bhandari, B. Dutta, H. Courtois, R. Fazio, F. Taddei, and J. P. Pekola, *Phys. Rev. B* **99**, 165405 (2019).
- [36] S.-Y. Hwang, R. López, and D. Sánchez, *Phys. Rev. B* **91**, 104518 (2015).
- [37] M. Tinkham, *Introduction to Superconductivity* (Dover Publications, Mineola, New York, 2004).
- [38] P.-G. de Gennes, in *Superconductivity of Metals and Alloys*, Advanced Book Classics (Perseus Books, Cambridge, 1999).
- [39] T. Wehling, A. Black-Schaffer, and A. Balatsky, *Adv. Phys.* **63**, 1 (2014).
- [40] G. D. Mahan, *Many-Particle Physics* (Kluwer Academic/Plenum Publishers, New York, 2000).
- [41] $I_R = -I_L$ due to charge conservation.
- [42] See Supplemental Material at <http://link.aps.org/supplemental/10.1103/PhysRevLett.124.106801> for a derivation of some of the results presented in the main text, including the discussion of additional models where the general conditions for thermoelectricity apply and an extended presentation of the applications mentioned in the main text, which includes Refs. [43–47].
- [43] P. Horowitz and W. Hill, *The Art of Electronics* (Cambridge University Press, Cambridge, England, 2015).
- [44] S. Strogatz, in *Nonlinear Dynamics and Chaos: With Applications to Physics, Biology, Chemistry and Engineering* (Westview Press, Cambridge, 1994).
- [45] G. Sansone, *Ann. Mat. Pura Appl.* **28**, 153 (1949).
- [46] M. Sabatini and G. Villari, *Matematiche* **LXV**, 201 (2010).
- [47] J. Stoker, *Nonlinear Vibrations in Mechanical and Electrical Systems* (Interscience Publishers, New York, 1950).

- [48] I. Prigogine, *Introduction to Thermodynamics of Irreversible Processes* (Thomas, Springfield, 1955).
- [49] S. R. de Groot and P. Mazur, *Non-Equilibrium Thermodynamics* (North-Holland, Amsterdam, 1962).
- [50] K. Yamamoto and N. Hatano, *Phys. Rev. E* **92**, 042165 (2015).
- [51] J. Bardeen, L. N. Cooper, and J. R. Schrieffer, *Phys. Rev.* **108**, 1175 (1957).
- [52] S. S. Pershoguba and L. I. Glazman, *Phys. Rev. B* **99**, 134514 (2019).
- [53] C. Guarcello, A. Braggio, P. Solinas, and F. Giazotto, *Phys. Rev. Applied* **11**, 024002 (2019).
- [54] The subgap transport in realistic junctions is accounted for with a small parameter Γ_α [55]. The DOS reads: $N_\alpha = |\text{Re}[(E + i\Gamma_\alpha)/\sqrt{(E + i\Gamma_\alpha)^2 - \Delta_\alpha^2}]|$. In the calculations we set $\Gamma_\alpha = 10^{-4}\Delta_{0,\alpha}$.
- [55] R. C. Dynes, J. P. Garno, G. B. Hertel, and T. P. Orlando, *Phys. Rev. Lett.* **53**, 2437 (1984).
- [56] A. G. Aronov and B. Z. Spivak, *JETP Lett.* **22**, 101 (1975), http://www.jetpletters.ac.ru/ps/1523/article_23302.shtml.
- [57] M. E. Gershenzon and M. I. Falei, *JETP Lett.* **44**, 682 (1986), http://www.jetpletters.ac.ru/ps/1398/article_21212.shtml.
- [58] M. E. Gershenzon and M. I. Falei, *Sov. Phys. JETP* **67**, 389 (1988), <http://www.jetp.ac.ru/cgi-bin/e/index/e/67/2/p389?a=list>.
- [59] J. G. Gijsbertsen and J. Flokstra, *J. Appl. Phys.* **80**, 3923 (1996).
- [60] J. Nagel, D. Speer, T. Gaber, A. Sterck, R. Eichhorn, P. Reimann, K. Ilin, M. Siegel, D. Koelle, and R. Kleiner, *Phys. Rev. Lett.* **100**, 217001 (2008).
- [61] C. Goupil, H. Ouerdane, E. Herbert, G. Benenti, Y. D'Angelo, and P. Lecoeur, *Phys. Rev. E* **94**, 032136 (2016).
- [62] R. Alicki, D. Gelbwaser-Klimovsky, and A. Jenkins, *Ann. Phys. (Amsterdam)* **378**, 71 (2017).